Appl. Math. Mech. -Engl. Ed., **33**(1), 51–64 (2012)
DOI 10.1007/s10483-012-1533-6

Applied Mathematics and Mechanics (English Edition)

MHD flow and heat transfer of micropolar fluid between two porous disks*

M. ASHRAF[1], A. R. WEHGAL[1,2]

(1. Centre for Advanced Studies in Pure and Applied Mathematics,
Bahauddin Zakariya University, Multan, Pakistan;
2. Department of Mathematics, Stockholm University, Stockholm, Sweden)

Abstract A numerical study is carried out for the axisymmetric steady laminar incompressible flow of an electrically conducting micropolar fluid between two infinite parallel porous disks with the constant uniform injection through the surface of the disks. The fluid is subjected to an external transverse magnetic field. The governing nonlinear equations of motion are transformed into a dimensionless form through von Karman's similarity transformation. An algorithm based on a finite difference scheme is used to solve the reduced coupled ordinary differential equations under associated boundary conditions. The effects of the Reynolds number, the magnetic parameter, the micropolar parameter, and the Prandtl number on the flow velocity and temperature distributions are discussed. The results agree well with those of the previously published work for special cases. The investigation predicts that the heat transfer rate at the surfaces of the disks increases with the increases in the Reynolds number, the magnetic parameter, and the Prandtl number. The shear stresses decrease with the increase in the injection while increase with the increase in the applied magnetic field. The shear stress factor is lower for micropolar fluids than for Newtonian fluids, which may be beneficial in the flow and thermal control in the polymeric processing.

Key words MHD flow, porous disk, micropolar fluid, heat transfer, microrotation

Chinese Library Classification O361.3, O368
2010 Mathematics Subject Classification 76A05, 76M20, 76W05, 80A20

1 Introduction

The fluid flow between parallel disks has significant importance due to its applications in a number of technological and engineering processes. Such type flows have applications in hydrodynamical machines and apparatus, semiconductor manufacturing processes with rotating wafers, magnetic storage devices (disk drives), gas turbine engines, computer storage devices, heat and mass exchanges, crystal growth processes, biomechanics, etc. Magnetohydrodynamics (MHD) is important in the magnetic confinement of plasmas in experiments of controlled thermonuclear fusion. MHD principles are used for MHD power generator, light-ion-beam powered inertial confinement, and ion thrusters for spacecraft propulsion. Elcrat[1] proved the theorem of existence and uniqueness for the non-rotational fluid motion between fixed porous disks with uniform arbitrary suction or injection. Rasmussen[2] numerically studied the problem of

* Received Mar. 16, 2011 / Revised Sept. 20, 2011
Corresponding author M. ASHRAF, Ph. D., E-mail: mashraf_mul@yahoo.com

the steady viscous symmetric flow between two parallel porous coaxial disks. The governing Navier-Stokes equation of motion was reduced to an ordinary differential equation in the dimensionless form by using a similarity transformation. Gaur and Chaudhary[3] discussed the problem of heat and mass transfer for the laminar flow between two parallel porous disks of different permeabilities. Rudraiah and Chandrasekhara[4] analyzed the MHD laminar flow between two parallel porous disks for large suction Reynolds numbers by using a perturbation technique. Phan-Thien and Bush[5] investigated the problem of the steady flow between two parallel disks by solving the reduced nonlinear algebraic system of equations by a standard optimization method. Attia[6] solved the problem of the steady flow and heat transfer of a conducting fluid due to the rotation of an infinite non-conducting porous disk in the presence of an external magnetic field by considering the ion slip. The fluid motion was superimposed by the uniform injection/suction through the surface of the porous disk. The self similar governing equations were solved numerically by using the finite difference discretization. Fang[7] presented an exact solution for the problem of the steady incompressible flow over a stretchable disk in the absence of body force by using an extension of Von Karman's similarity transformation to discuss the effects of disk stretching and rotation. Ibrahim[8] investigated the unsteady flow of a viscous incompressible fluid between two parallel rotating disks. The governing momentum and energy equations were transformed to a set of ordinary differential equations through a similarity transformation. It was concluded that the rotation of the two disks has a very small effect on the fluid temperature and heat transfer process, while rapid normal motion of the upper disk has a dominant effect on the temperature of the fluid and the heat transfer process. Frusteri and Osalusi[9] investigated the MHD steady laminar flow of a viscous electrically conducting fluid over a rotating porous disk with the slip boundary condition to discuss the variable fluid properties (density and viscosity). The governing partial differential equations were transformed to ordinary ones by using von Karman's similarity transformation and were solved numerically by using a shooting method. Ersoy[10] investigated an approximate solution of the flow of a linearly viscous fluid between two disks rotating about two distinct vertical axes to show the dependence of the velocity components on the position, the Reynolds number, the eccentricity, and the ratio of angular speeds of the disks.

In all the studies cited above, the authors are confined to the Newtonian fluids only. However, many of the fluids involved in technical processes and engineering applications exhibit non-Newtonian behaviors. The classical Newtonian model is inadequate to describe some modern engineering structures, which are made up of materials processing an internal structure, e.g., polycrystalline materials, fluids containing additives, and the materials with fibrous or coarse grain structures. Eringen[11–12] introduced that the deformation of such materials can be well explained by one of the best theories of micropolar fluids. This theory can describe the mathematical model for non-Newtonian fluids, which can be used to study the behaviors of exotic lubricants, polymeric suspensions, muddy and biological fluids, animal blood, colloidal solutions, liquid crystals with rigid molecules, etc. Airman et al.[13] presented a comprehensive review of the micropolar fluid theory and its application. Guram and Anwar[14] discussed numerically the problem of the steady incompressible flow of a micropolar fluid between a rotating and a stationary disk by using an algorithm based on the finite difference approximation. Guram and Anwar[15] numerically solved the problem of the steady laminar incompressible flow of a micropolar fluid due to a rotating disk with injection/suction. Takhar et al.[16] presented the finite element solution of the steady flow and heat transfer of an incompressible micropolar fluid between two porous disks. Wang and Zhu[17] studied numerically the non-Newtonian behavior of journal bearings lubricated with micropolar fluids considering both thermal and cavitating effects. They concluded that micropolar fluids exhibited increases in the load capacity and temperature while decreases in the coefficient of the friction and side leakage flow. Sacheti and Bhatt[18] examined the problem of heat transfer of the steady laminar flow of a non-Newtonian fluid between two infinite parallel circular porous disks with injection/suction through the disks.

Anwar-Kamal et al.[19] presented the numerical investigations of the steady symmetric flow of a micropolar fluid between two porous co-axial disks. Ashraf et al.[20] numerically investigated the problem of the two-dimensional steady laminar and incompressible flow of a micropolar fluid between a permeable and an impermeable disk to discuss the influence of the Reynolds number and the micropolar structure on the flow characteristics. Ashraf et al.[21] considered the numerical study of the asymmetric steady laminar incompressible flow of a micropolar fluid in a porous channel having walls with different permeabilities.

The purpose of the present paper is to present a comprehensive parametric study of the flow and heat transfer of a steady incompressible viscous electrically conducting micropolar fluid between two stationary infinite parallel porous disks in the presence of a uniform magnetic field which has not been considered by previous authors. A numerical solution is obtained for the governing momentum, the angular momentum, and the energy equations by using an algorithm based on finite difference approximations.

2 Problem formulation

Consider the axisymmetric steady laminar incompressible flow of an electrically conducting micropolar fluid between two parallel stationary porous disks of infinite radii located at the planes $z = \pm a$ shown in Fig. 1. A uniform transverse magnetic field of the strength B_0 is applied at the disks. We assume a uniform stationary magnetic field B in the transverse direction, which is perpendicular to the velocity field V lying in the rz-plane. The induced magnetic field b is negligible as compared with the imposed field. The magnetic Reynolds number $Re_{\mathrm{M}} = LU/\eta_0$ is small[22], where L is a characteristic length of the fluid, U is the fluid velocity, and η_0 is the magnetic diffusivity. It is used to compare the transport of the magnetic lines of force in a conducting fluid with the leakage of such lines from the fluid. For small Re_{M}, the magnetic field will tend to relax towards a purely diffusive state. It is assumed that there is no applied polarization voltage, i.e., the electric field $E = 0$. The electrical current flowing in the fluid will give rise to an induced magnetic field, which exists if the fluid is an electrical insulator. Here, the fluid is to be electrically conducting. In view of the above assumptions, the electromagnetic body force has the linearized form, i.e., $-\sigma_{\mathrm{e}} B_0^2 V$[23].

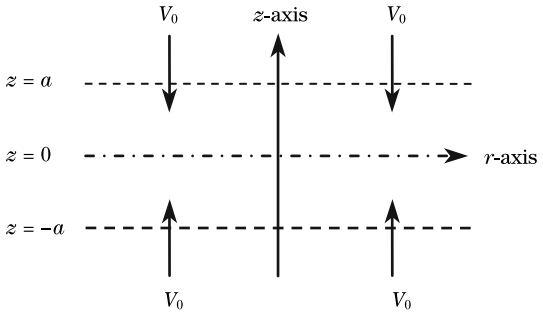

Fig. 1 Geometry of disks

Following Eringen[11–12], the governing equations of motion for the MHD steady laminar viscous incompressible flow of a micropolar fluid are

$$\frac{\partial u}{\partial r} + \frac{u}{r} + \frac{1}{a}\frac{\partial w}{\partial \eta} = 0, \tag{1}$$

$$\rho\Big(u\frac{\partial u}{\partial r} + \frac{w}{a}\frac{\partial u}{\partial \eta}\Big) = -\frac{\partial p}{\partial r} - \frac{\kappa}{a}\frac{\partial v_2}{\partial \eta} - \sigma_{\mathrm{e}} B_0^2 u + (\mu + \kappa)\Big(\frac{\partial^2 u}{\partial r^2} + \frac{1}{r}\frac{\partial u}{\partial r} - \frac{u}{r^2} + \frac{1}{a^2}\frac{\partial^2 u}{\partial \eta^2}\Big), \tag{2}$$

$$\rho\Big(u\frac{\partial w}{\partial r}+\frac{w}{a}\frac{\partial w}{\partial \eta}\Big)=-\frac{1}{a}\frac{\partial p}{\partial \eta}+\kappa\Big(\frac{\partial \upsilon_2}{\partial r}+\frac{\upsilon_2}{r}\Big)$$
$$+(\mu+\kappa)\Big(\frac{\partial^2 w}{\partial r^2}+\frac{1}{r}\frac{\partial w}{\partial r}+\frac{1}{a^2}\frac{\partial^2 w}{\partial \eta^2}\Big), \tag{3}$$

$$\rho j\Big(u\frac{\partial \upsilon_2}{\partial r}+\frac{w}{a}\frac{\partial \upsilon_2}{\partial \eta}\Big)=\kappa\Big(\frac{1}{a}\frac{\partial u}{\partial \eta}-\frac{\partial w}{\partial r}\Big)-2\kappa\upsilon_2$$
$$+\gamma\Big(\frac{\partial^2 \upsilon_2}{\partial r^2}+\frac{1}{r}\frac{\partial \upsilon_2}{\partial r}-\frac{\upsilon_2}{r^2}+\frac{1}{a^2}\frac{\partial^2 \upsilon_2}{\partial \eta^2}\Big), \tag{4}$$

$$\nabla\cdot B=0, \tag{5}$$

$$\nabla\times B=\mu_{\mathrm{m}}J, \tag{6}$$

$$\nabla\times E=0, \tag{7}$$

$$J=\sigma_{\mathrm{e}}(E+V\times B), \tag{8}$$

where η is the similarity variable. V is the fluid velocity vector. (u, v, w) and $(\upsilon_1,\ \upsilon_2,\ \upsilon_3)$ are the components of the velocity and the microrotation, respectively. ρ is the density. p is the pressure. j is the microinertia. J is the current density. μ_{m} is the magnetic permeability. E is the electric field. B is the total magnetic field satisfying $B=B_0+b$, where b is the induced magnetic field. σ_{e} is the electrical conductivity of the fluid. μ is the dynamic viscosity. κ is the vortex viscosity of the fluid. Furthermore, $\nabla\cdot J=0$ is obtained from Eqs. (5) and (6). Here, the velocity vector V and υ are unknown microrotation vectors.

The components of the velocity (u, v, w) and the microrotation $(\upsilon_1,\ \upsilon_2,\ \upsilon_3)$ along the radial, transverse, and axial directions can be written as

$$\begin{cases} u=u(r,z), \quad v=0, \quad w=w(r,z), \\ \upsilon_1=0, \quad \upsilon_2=\upsilon_2(r,z), \quad \upsilon_3=0. \end{cases} \tag{9}$$

The equation for the temperature field, neglecting the viscous dissipation, can be written as

$$\rho c_p\Big(u\frac{\partial T}{\partial r}+\frac{w}{a}\frac{\partial T}{\partial \eta}\Big)-\kappa_0\Big(\frac{1}{a^2}\frac{\partial^2 T}{\partial \eta^2}+\frac{\partial^2 T}{\partial r^2}+\frac{1}{r}\frac{\partial T}{\partial r}\Big)=0, \tag{10}$$

where $\eta=z/a$, T is the temperature, c_p is the specific heat at the constant pressure, and κ_0 is the thermal conductivity of the fluid. The boundary conditions at the two porous disks for the velocity field are

$$u(r,\pm 1)=0, \quad w(r,\pm 1)=\mp V_0, \tag{11}$$

where V_0 is a constant injection velocity at the disks.

Following Ref. [16], the no-spin boundary conditions at the boundaries for the microrotation are given by

$$(\upsilon_1,\upsilon_2,\upsilon_3)=(0,0,0) \quad \text{at} \quad \eta=\pm 1. \tag{12}$$

The boundary conditions for the temperature field can be written as

$$T=\begin{cases} T_1, & \eta=-1, \\ T_2, & \eta=1. \end{cases} \tag{13}$$

To obtain the velocity, microrotation, and temperature fields for the present problem, we have to solve Eqs. (1)–(4) and (10) subjected to the boundary conditions given in Eqs. (11)–(13). For this purpose, we use the following similarity transformation similar to those of Takhar et al.[16], Ashraf et al.[20], von Karman[24], and Elkouh[25]:

$$\Psi(r,\eta) = \frac{V_0 r^2}{2} f(\eta) \tag{14}$$

so that

$$u = \frac{1}{ra}\frac{\partial \psi}{\partial \eta} = \frac{V_0 r}{2a} f'(\eta), \tag{15}$$

$$w = -\frac{1}{r}\frac{\partial \psi}{\partial r} = -V_0 f(\eta), \tag{16}$$

$$v_2 = \frac{V_0 r}{2a^2} g(\eta), \tag{17}$$

$$\theta(\eta) = \frac{T - T_1}{T_2 - T_1}. \tag{18}$$

The velocity components given in Eqs. (15) and (16) satisfy the continuity Eq. (1), and hence represent a possible fluid motion. Using Eqs. (15)–(18) in the governing equations (2)–(4), we get the following equations in the dimensionless form:

$$(1+R)f'''' + Re(ff''' - M^2 f'') - Rg'' = 0, \tag{19}$$

$$Cg'' - ARe\Big(\frac{1}{2}f'g - fg'\Big) + R(f'' - 2g) = 0, \tag{20}$$

$$\theta'' + RePrf\theta' = 0, \tag{21}$$

where

$$Re = \frac{\rho V_0 a}{\mu}, \quad M = \sqrt{\frac{\sigma_e a B_0^2}{\rho V_0}}, \quad R = \frac{\kappa}{\mu}, \quad A = \frac{j}{a^2}, \quad C = \frac{\gamma}{\mu a^2}, \quad Pr = \frac{\mu\, c_p}{\kappa_0}$$

are the Reynolds number, the magnetic parameter, the vortex viscosity parameter, the microinertia density parameter, the spin gradient viscosity parameter, and the Prandtl number, respectively. Here, R, A, and C are micropolar parameters. For the present problem, we will discuss the injection case, i.e., $Re < 0$. Integrating Eq. (19) w.r.t η, we get

$$(1+R)f''' + Re\Big(ff'' - \frac{f'^2}{2} - M^2 f'\Big) - Rg' = B, \tag{22}$$

where B is a constant of integration.

The boundary conditions (11)–(13) in the dimensionless form can be written as

$$\begin{cases} f(\pm 1) = \pm 1, \quad f'(\pm 1) = 0, \\ g(\pm 1) = 0, \\ \theta(-1) = 0, \quad \theta(1) = 1. \end{cases} \tag{23}$$

The shear and couple stresses on the disks are defined, respectively, as

$$\tau_\omega = -(\mu+\kappa)\frac{\partial u}{\partial z}\Big|_{z=\pm a} = -\mu(1+R)\frac{rV_0}{2a^2}f''(\pm 1), \tag{24}$$

$$m_\omega = -\gamma\frac{\partial v}{\partial z}\Big|_{z=\pm a} = -\gamma\frac{rV_0}{2a^3}g'(\pm 1). \tag{25}$$

We have to solve the system of Eqs. (20)–(22) subjected to the boundary conditions (23). It can be noted that Eqs. (20)–(22) reduce to the corresponding equations for the Newtonian fluid flow between two porous disks in the absence of a magnetic field obtained by Rasmussen[2] and Elkouh[25] for vanishing microrotation with $R = 0$ and $M = 0$. Furthermore, these equations together with the associated boundary condition (23) are inline with those obtained by Takhar et al.[16] in the absence of the external magnetic field, i.e., $M = 0$. These facts validate our model for the micropolar fluid motion in the presence of the external magnetic field.

3 Numerical solution

The reduced ordinary differential equations (20)–(22) are highly nonlinear and difficult to be solved analytically. We seek a numerical solution to these equations subjected to the associated boundary condition (23) by using a finite difference scheme. The order of the momentum equation (20) can be reduced by substituting $q = f'$ within it. Now, we have to solve the boundary value problem consisting of the following equations:

$$q = f' = \frac{\mathrm{d}f}{\mathrm{d}\eta}, \tag{26}$$

$$(1+R)q'' + Re\Big(fq' - \frac{q^2}{2} - M^2 q\Big) - Rg' = B, \tag{27}$$

$$Cg'' - ARe\Big(\frac{q}{2}g - fg'\Big) + R(q' - 2g) = 0, \tag{28}$$

$$\theta'' + RePrf\theta' = 0 \tag{29}$$

subjected to the boundary conditions

$$\begin{cases} f(\pm 1) = \pm 1, \quad q(\pm 1) = 0, \\ g(\pm 1) = 0, \quad \theta(-1) = 0, \quad \theta(1) = 1. \end{cases} \tag{30}$$

For the numerical solution to the above boundary value problem, we discretize the domain $[-1, 1]$ uniformly with the step h. Simpson's rule[26] with the formula given by Milne[27] is used to integrate Eq. (27). The central difference approximations are used to discretize Eqs. (27)–(29) at a typical grid point $\eta = \eta_n$ in the interval $[-1, 1]$. A successive over relaxation (SOR) parameter method is used to solve iteratively the system of the discrete equations subjected to the associated boundary conditions (30). The solution procedure, which is mainly based on the algorithm described by Syed et al.[28], is used to accelerate the iterative procedure and to improve the accuracy of the solution.

The iterative procedure is stopped if the following criterion is satisfied for four consecutive iterations:

$$\max(\|q^{(i+1)} - q^{(i)}\|_2,\ \|g^{(i+1)} - g^{(i)}\|_2,\ \|f^{(i+1)} - f^{(i)}\|_2,\ \|\theta^{(i+1)} - \theta^{(i)}\|_2) < e_{\mathrm{tol}}. \tag{31}$$

Here, e_{tol} is the prescribed error tolerance. We have taken at least 10^{-12} for it during the execution of a computer program in FORTRAN 90. The higher-order accuracy of the approximations to the exact solutions can be obtained by the use of Richardson's extrapolation. This process can be carried out by using Deuflhard's extrapolation scheme[29].

4 Results and discussion

The aim of the present study is to investigate numerically the flow and heat transfer characteristics associated with the steady laminar incompressible viscous flow of a micropolar fluid between two parallel porous disks in the presence of a uniform magnetic field. In this section, we present a comprehensive numerical study of our findings in tabular and graphical forms together with the discussion and their interpretations. To develop better understanding of the influences of the micropolar structure of the electrically conducting fluids and the permeability of the porous disks on the flow and thermal characteristics, we choose to present the shear and couple stresses at the two disks and the velocity, temperature, and microrotation fields across the disks for a range of the Reynolds number Re, the magnetic parameter M, the micropolar parameter R, and the Prandtl number Pr. The results are computed for three grid sizes, i.e., $h = 0.02$, 0.01, 0.005 for the stability of our numerical scheme, and then extrapolated on finer grids by using Richardson's extrapolation.

A comparison of the numerical values of the dimensionless temperature $\theta(\eta)$ for three grid sizes and their extrapolated values is given in Table 1. An excellent agreement is observed, which validates our numerical computation. Other sources of validity of our numerical results are listed in Tables 2 and 3, in which the present results for the shear and couple stresses at the disks are compared with the published literature results given by Takhar et al.[16] in the absence of the magnetic field. The results show a good agreement. The arbitrary values 0, 4, 8, 12, and 16 of the micropolar parameter R are taken to discuss its effect on the flow behavior as done customararily in Refs. [15–16, 30–32]. It has been noticed that the other two micropolar parameters A and C have no significant effect on the velocity and thermal fields. Therefore, their values are fixed as $A = 1$ and $C = 2$ throughout the study as done by Takhar et al.[16], Chang[30], and Lok et al.[31].

Table 1 Dimensionless temperature $\theta(\eta)$ on three grid sizes and extrapolated values for $Re = -20$, $M = 0.4$, and $Pr = 0.2$

η	$\theta(\eta)$			
	$h = 0.02$	$h = 0.01$	$h = 0.005$	Extrapolated value
−1.0	0.000 000	0.000 000	0.000 000	0.000 000
−0.8	0.022 782	0.022 797	0.022 800	0.022 802
−0.6	0.071 236	0.071 263	0.071 271	0.071 273
−0.4	0.163 486	0.163 516	0.163 524	0.163 526
−0.2	0.311 034	0.311 046	0.311 049	0.311 051
0.0	0.500 039	0.500 018	0.500 014	0.500 013
0.2	0.689 034	0.688 986	0.688 975	0.688 971
0.4	0.836 561	0.836 506	0.836 493	0.836 489
0.6	0.928 789	0.928 748	0.928 738	0.928 735
0.8	0.977 227	0.977 208	0.977 203	0.977 201
1.0	1.000 000	1.000 000	1.000 000	1.000 000

Table 2 Comparison of numerical values of shear stress $-f''(1)$ for $M = 0$, $Pr = 0.1$, and various R and Re

R	Re			
	−10		−5	
	Present	Ref. [16]	Present	Ref. [16]
5	2.264 02	2.263 92	2.382 72	2.382 59
10	2.146 91	2.146 73	2.217 13	2.216 95

Table 3 Comparison of numerical values of couple stress $g'(1)$ for $M = 0$, $Pr = 0.1$, and various R and Re

R	Re			
	-10		-5	
	Present	Ref. [16]	Present	Ref. [16]
5	3.083 25	3.083 49	3.122 09	3.122 32
10	4.753 61	4.754 31	4.811 64	4.812 37

From Fig. 2, it is noted that micropolar fluids reduce the shear stresses and increase the couple stresses as compared with Newtonian fluids, which may be beneficial in the flow control of the polymeric processing. This is due to the reason that micropolar fluids offer a greater resistance resulting from the dynamic viscosity and vortex viscosity to the fluid motion as compared with Newtonian fluids.

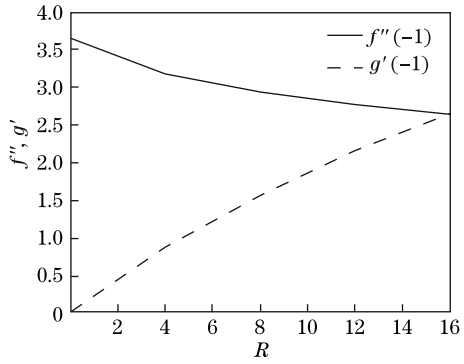

Fig. 2 Shear and couple stresses at lower disk for various R with $Re = -10$, $M = 1.5$, and $Pr = 0.2$

Now, we investigate the influence of the Reynolds number Re on the shear stress $f''(-1)$, the couple stress $g'(-1)$, and the heat transfer rate $\theta'(-1)$ at the lower disk. From Figs. 3 and 4, it can be noted that the shear and couple stresses and the heat transfer rate at the disks decrease as the injection increases. The heat transfer rate at the disks approaches zero as $Re \to -\infty$.

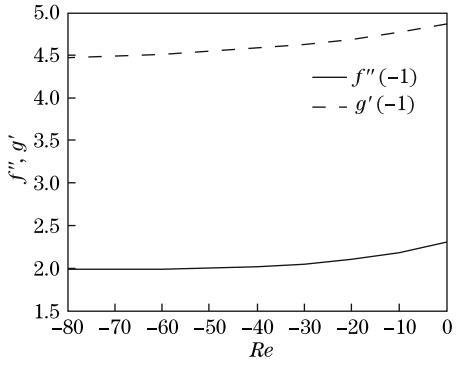

Fig. 3 Shear and couple stresses at lower disk for various Re with $M = 0.4$, $Pr = 0.2$, and $R = 10$

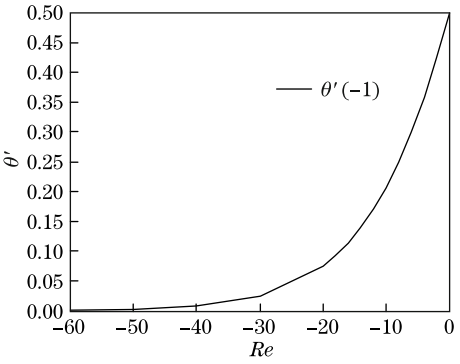

Fig. 4 Heat transfer rate at lower disk for various Re with $M = 0.4$, $Pr = 0.2$, and $R = 10$

The influences of the imposition of the external magnetic field on the shear and couple stress and the heat transfer rate at the disk are given in Figs. 5(a) and 5(b). The applied magnetic

field enhances the values of the shear and couple stresses and the heat transfer rate for fixed values of the Reynolds number Re, the micropolar parameter R, and the Prandtl number Pr. It is shown in Fig. 6 that the heat transfer rate decreases with the increases in the Prandtl number Pr. The shear and couple stresses are unaffected by the variation of Pr. Due to the symmetry, the results in Figs. 2–6 are given at the lower disk only.

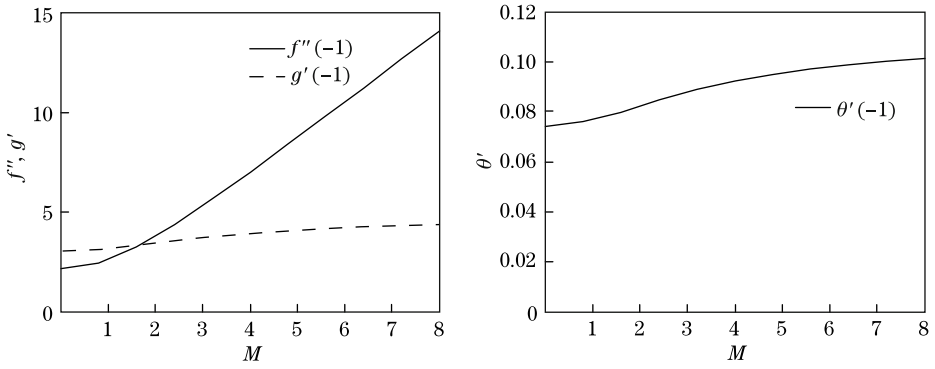

(a) Shear and couple stress (b) Heat transfer rate

Fig. 5 Shear and couple stresses and heat transfer rate at lower disk for various M with $Re = -20$, $Pr = 0.2$, and $R = 5$

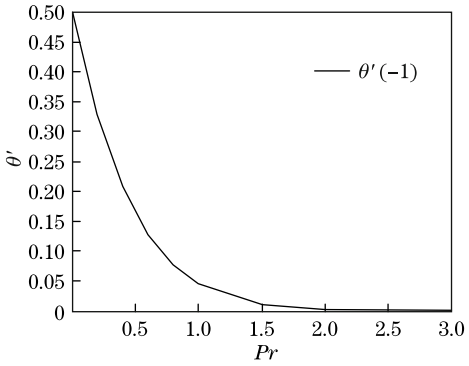

Fig. 6 Heat transfer rate at lower disk for various Pr with $Re = -50$, $M = 0.4$, and $R = 3$

Now, we give graphical interpretations for the velocity and thermal fields and the microrotation across the disks. The influence of the Reynolds number on the axial velocity is presented in Fig. 7. As a general trend, the axial velocity takes its dimensionless value 1 at the upper disk and -1 at the lower disk with a point of inflection on the central plane $z = 0$, where the concavity is changed. The axial velocity profiles given in Fig. 7 help in finding the position of the viscous layer, which is developed due to the injection at the disks. The position of the viscous layer is a point, where $f(\eta) = 0$. In the present problem for the symmetric flow between two porous disks, this layer coincides with the central plane $z = 0$. However, the position of this viscous layer moves away from the plane $z = 0$ for the asymmetric flow. A slight increase near the upper disk and a slight decrease near the lower disk in f are noted with an increase in the magnitude of Re. This reflects the effect of the increase in the injection velocity on the axial velocity component in view of the fact that injection will assist the axial velocity near the lower disk and resist the axial velocity near the upper disk. The effect of the Reynolds number

Re on the radial velocity is given in Fig. 8 for a set of values of the magnetic parameter M, the micropolar parameter R, and the Prandtl number Pr. As the imposed injection through the disks increases, the fluid is pushed towards the central region between the disks, and therefore the radial velocity increases significantly with the increase in Re in the magnitude. Figure 9 reveals the microrotation for various values of Re. The microrotation has opposite signs near the disks. The shear stresses at the two disks tend to rotate the fluid in opposite directions, and the point of zero microrotation marks the position across the disks where the effects of the opposite rotations balance each other. An increase in the magnitude of the microrotation is observed with an increase in the values of the magnitude of Re. An increase in the temperature in the upper region of the plane $z = 0$ and a decrease in the temperature in the lower region are observed with the increased injection as shown in Fig. 10.

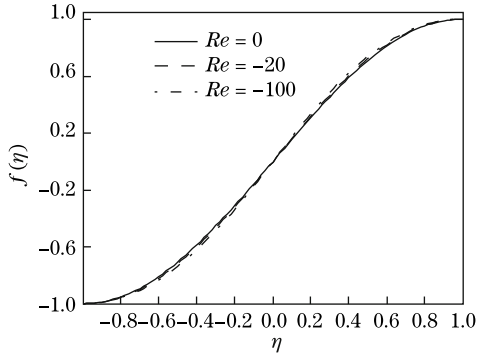

Fig. 7 Dimensionless axial velocity $f(\eta)$ for various Re with $R = 10$, $M = 0.4$, and $Pr = 0.2$

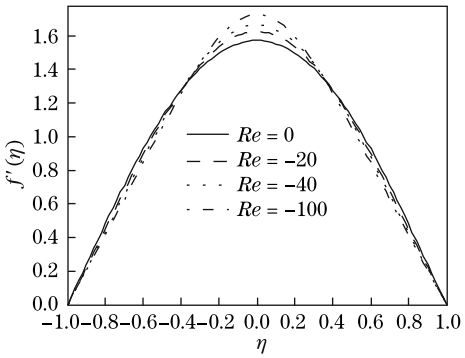

Fig. 8 Dimensionless radial velocity $f'(\eta)$ for various Re with $R = 10$, $M = 0.4$, and $Pr = 0.2$

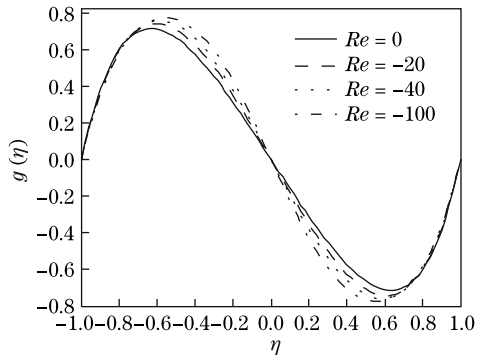

Fig. 9 Dimensionless microrotation $g(\eta)$ for various Re with $R = 10$, $M = 0.4$, and $Pr = 0.2$

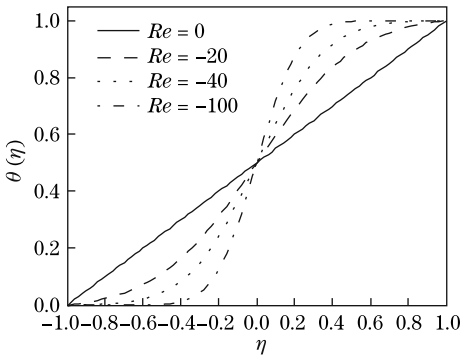

Fig. 10 Dimensionless temperature $\theta(\eta)$ for various Re with $R = 10$, $M = 0.4$, and $Pr = 0.2$

Figures 11–14 depict the influence of the external applied magnetic field on the flow velocities, the microrotation, and the temperature, respectively. From Fig. 11, it is clear that the axial velocity profiles rise near the lower disk and fall near the upper disk by increasing the values of the magnetic parameter M. Opposite to the effect of the Reynolds number Re, the radial velocity decreases near the central plane and the fluid is pushed towards the boundaries by increasing M, as shown in Fig. 12. Furthermore, the radial velocity is parabolic for small values of the magnetic parameter M. As M increases, the radial velocity exhibits the charac-

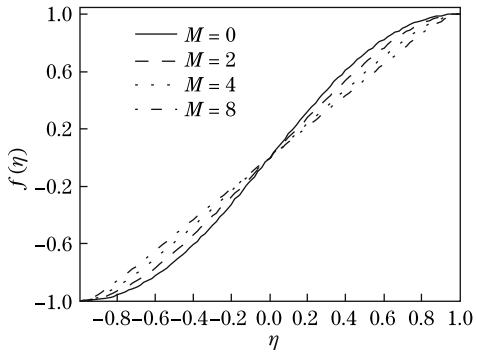

Fig. 11 Dimensionless axial velocity $f(\eta)$ for various M with $R = 5$, $Re = -20$, and $Pr = 0.2$

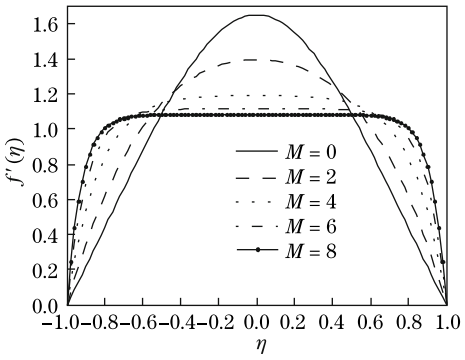

Fig. 12 Dimensionless radial velocity $f'(\eta)$ for various M with $R = 5$, $Re = -20$, and $Pr = 0.2$

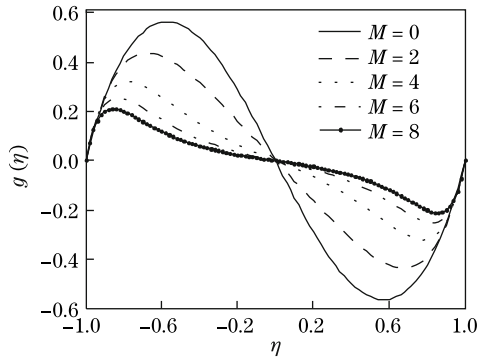

Fig. 13 Dimensionless microrotation $g(\eta)$ for various M with $R = 5$, $Re = -20$, and $Pr = 0.2$

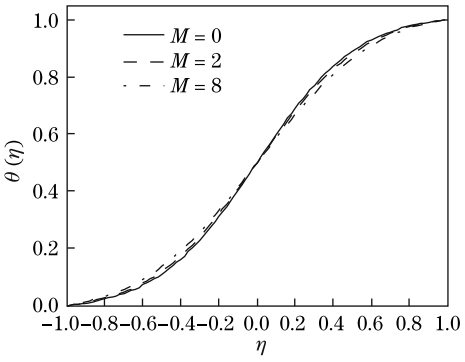

Fig. 14 Dimensionless temperature $\theta(\eta)$ for various M with $R = 5$, $Re = -20$, and $Pr = 0.2$

teristic flattering. From Fig. 13, we see that the values of the microrotation are positive in the first half region and negative in the second half region, which shows a reverse rotation near the boundaries of the two disks. Due to the damping effects, the magnitude of the microrotation decreases with the increase in M, which shows that the intensity of the applied magnetic field can be used to decrease the angular rotation arising in lubrication problems, especially in suspension flows. Figure 14 plots the variation of the dimensionless temperature as a function of η for different M and fixed Re, R, and Pr. It can be seen that the temperature of the fluid increases throughout with the increase in η for a given M. The temperature profiles increase near the lower disk while decrease near the upper disk with the increase in M.

Figures 15–17 illustrate the influence of the micropolar parameter R on the velocity and microrotation fields. The axial velocity $f(\eta)$ increases throughout from -1 to 1 for a given value of R as shown in Fig. 15. Figure 16 depicts the behavior of the radial velocity for different R. The radial velocity profiles are parabolic in nature for all the values of the micropolar parameter R. The radial velocity increases near the central plane, while its profiles fall near the boundaries of the disks with an increase in the values of R. Figure 17 presents the effect of the micropolar parameter R on the microrotation for $Re = -10$, $M = 1.5$, and $Pr = 0.2$. The case for $R = 0$ corresponds to the Newtonian fluids. It is seen that there is no microrotation in this case while there are significant influences on the microrotation for the other cases. The magnitude of the microrotation increases by the increase in the values of R. The variation of

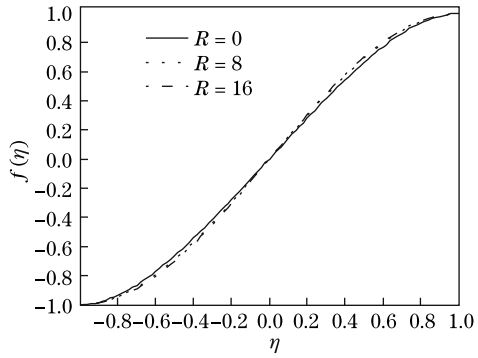

Fig. 15 Dimensionless axial velocity $f(\eta)$ for various R with $Re = -10$, $M = 1.5$, and $Pr = 0.2$

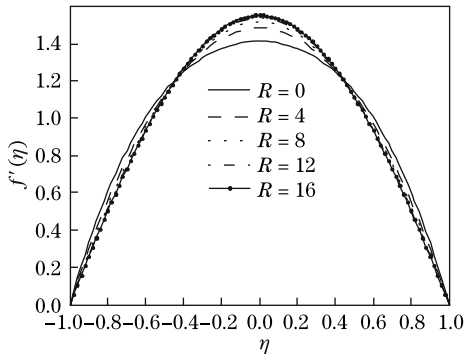

Fig. 16 Dimensionless radial velocity $f'(\eta)$ for various R with $Re = -10$, $M = 1.5$, and $Pr = 0.2$

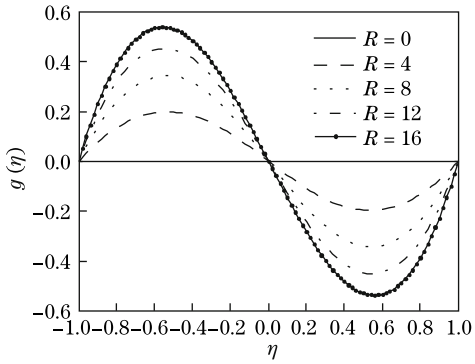

Fig. 17 Dimensionless microrotation $g(\eta)$ for various R with $Re = -10$, $M = 1.5$, and $Pr = 0.2$

R has no significant effect on the temperature.

Figure 18 illustrates the variation of the dimensionless temperature $\theta(\eta)$ for selected values of the Prandtl number Pr. An increase in the values of Pr results in the increase in the temperature profiles in a region towards the right of the central plane $z = 0$, whereas results in the decrease in temperature profiles in a region towards the left of $z = 0$.

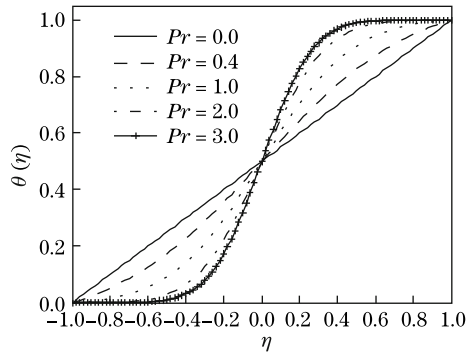

Fig. 18 Dimensionless temperature $\theta(\eta)$ for various Pr with $Re = -50$, $M = 0.2$, and $R = 3$

5 Conclusions

The present study has investigated the effects of some governing parameters on the flow of an electrically conducting micropolar fluid in the presence of an applied magnetic field. Numerical solutions of the transformed self similar governing equations and the associated boundary conditions have been obtained by using the finite difference discretization method. The following conclusions can be made:

(i) Micropolar fluids reduce the shear stresses as compared with Newtonian fluids.

(ii) The magnetic field enhances the shear stresses, the couple stresses, and the heat transfer rate.

(iii) The shear stresses and the heat transfer rate decrease by imposed injection.

(iv) The heat transfer rate decreases by the increase in the Prandtl number.

(v) The radial velocity increases near the central plane by increasing the Reynolds number and the micropolar parameter, whereas decreases near the central plane in the case of an increased magnetic field.

(vi) The magnitude of the microrotation increases with an increase in the values of the Reynolds number and the micropolar parameter, whereas it decreases in the case of increasing the values of the magnetic parameter.

Acknowledgements The authors wish to express their sincere thanks to the honorable referees for their valuable comments to improve the quality of the paper.

References

[1] Elcrat, A. R. On the radial flow of a viscous fluid between porous disks. *Archive for Rational Mechanics and Analysis*, **61**(1), 91–96 (1976)

[2] Rasmussen, H. Steady viscous flow between two porous disks. *Zeitschrift für Angewandte Mathematik und Physik*, **21**(2), 187–195 (1970)

[3] Guar, Y. N. and Chaudhary, R. C. Heat transfer for laminar flow through parallel porous disks of different permeability. *Proceedings Mathematical Sciences*, **87**(9), 209–217 (1978)

[4] Rudraiah, N. and Chandrasekhara, B. C. Flow of a conducting fluid between porous disks for large suction Reynolds number. *Journal of the Physical Society of Japan*, **27**, 1041–1045 (1969)

[5] Phan-Thien, N. and Bush, M. B. On the steady flow of a Newtonian fluid between two parallel disks. *Zeitschrift für Angewandte Mathematik und Physik*, **35**(6), 912–919 (1984)

[6] Attia, H. A. On the effectiveness of the ion slip on the steady flow of a conducting fluid due to a porous rotating disk with heat transfer. *Tamkang Journal of Science and Engineering*, **9**(3), 185–193 (2006)

[7] Fang, T. Flow over a stretchable disk. *Physics of Fluids*, **19**(2), 128105 (2007)

[8] Ibrahim, F. N. Unsteady flow between two rotating disks with heat transfer. *Journal of Physics D: Applied Physics*, **24**(8), 1293–1299 (1991)

[9] Frusteri, F. and Osalausi, E. On MHD and slip flow over a rotating porous disk with variable properties. *International Communications in Heat and Mass Transfer*, **34**(4), 492–501 (2007)

[10] Ersoy, H. V. An approximate solution for flow between two disks rotating about distinct axes at different speeds. *Mathematical Problems in Engineering*, **2007**, 1–16 (2007)

[11] Eringen, A. C. Simple microfluids. *International Journal of Engineering Science*, **2**(2), 205–217 (1964)

[12] Eringen, A. C. Theory of micropolar fluids. *Journal of Applied Mathematics and Mechanics*, **16**(1), 1–18 (1966)

[13] Ariman, T., Turk, M. A., and Sylvester, N. D. Microrotation fluid mechanics — a review. *International Journal of Engineering Science*, **11**, 905–930 (1973)

[14] Guram, G. S. and Anwar, M. Steady flow of a micropolar fluid due to a rotating disk. *Journal of Engineering Mathematics*, **13**(3), 223–234 (1979)

[15] Guram, G. S. and Anwar, M. Micropolar flow due to a rotating disk with suction and injection. *Zeitschrift für Angewandte Mathematik und Mechanik*, **61**(11), 589–605 (1981)

[16] Takhar, H. S., Bhargava, R., Agrawal, R. S., and Balaji, A. V. S. Finite element solution of micropolar fluid flow and heat transfer between two porous disks. *International Journal of Engineering Science*, **38**(17), 1907–1922 (2000)

[17] Wang, X. L. and Zhu, K. Q. Numerical analysis of journal bearings lubricated with micropolar fluids including thermal and cavitating effects. *Tribology International*, **39**(3), 227–237 (2006)

[18] Sacheti, N. C. and Bhatt, B. S. Steady laminar flow of a non-Newtonian fluid with suction or injection and heat transfer through porous parallel disks. *Zeitschrift für Angewandte Mathematik und Mechanik*, **56**(1), 43–50 (2006)

[19] Anwar-Kamal, M., Ashraf, M., and Syed, K. S. Numerical solution of steady viscous flow of a micropolar fluid driven by injection between two porous disks. *Applied Mathematics and Computation*, **179**(1), 1–10 (2006)

[20] Ashraf, M., Anwar-Kamal, M., and Syed, K. S. Numerical simulation of flow of a micropolar fluid between a porous disk and a non-porous disk. *Applied Mathematical Modelling*, **33**(4), 1933–1943 (2009)

[21] Ashraf, M., Anwar-Kamal, M., and Syed, K. S. Numerical study of asymmetric laminar flow of micropolar fluids in a porous channel. *Computers and Fluids*, **38**(10), 1895–1902 (2009)

[22] Shercliff, J. A. *A Text Book of Magnetohydrodynamics*, Pergamon Press, Oxford (1965)

[23] Rossow, V. J. *On Flow of Electrically Conducting Fluids Over a Flat Plate in the Presence of a Transverse Magnetic Field*, Report-1358, National Advisory Committee for Aeronautics, California (1958)

[24] Von Karman, M. Under laminare and turbulente Reibung. *Zeitschrift für Angewandte Mathematik und Mechanik*, **1**(4), 233–235 (1921)

[25] Elkouh, A. F. Laminar flow between porous disks. *Journal of the Engineering Mechanics Division*, **93**(4), 31–38 (1967)

[26] Gerald, C. F. *Applied Numerical Analysis*, Addison-Wesley Publishing Company, Massachusetts (1974)

[27] Milne, W. E. *Numerical Solutions of Differential Equations*, John Willey and Sons Inc., New York (1953)

[28] Syed, K. S., Tupholme, G. E., and Wood, A. S. Iterative solution of fluid flow in finned tubes. *Proceedings of the* 10*th International Conference on Numerical Methods in Laminar and Turbulent Flow* (eds. Taylor, C. and Cross, J. T.), Pineridge Press, Swansea, 429–440 (1997)

[29] Deuflhard, P. Order and step size control in extrapolation methods. *Numerische Mathematik*, **41**(3), 399–422 (1983)

[30] Chang, L. C. Numerical simulation of micropolar fluid flow along a flat plate with wall conduction and buoyancy effects. *Journal of Physics D*: *Applied Physics*, **39**(6), 1132–1140 (2006)

[31] Lok, Y. Y., Pop, I., and Chamkha, A. J. Nonorthogonal stagnation-point flow of a micropolar fluid. *International Journal of Engineering Science*, **45**(1), 173–184 (2007)

[32] Ashraf, M. and Ashraf, M. M. MHD stagnation point flow of a micropolar fluid towards a heated surface. *Applied Mathematics and Mechanics* (*English Edition*), **32**(1), 45–54 (2011) DOI 10.1007/s10483-011-1392-7